Temperature Effects in Adhesively Bonded FRP Strengthening Applied to Steel Beams

TEMPERATURE EFFECTS IN ADHESIVELY BONDED FIBRE-REINFORCED POLYMER STRENGTHENING APPLIED TO STEEL BEAMS

Dr Tim Stratford, Dr Luke Bisby
Joint Research Institute for Civil and Environmental Engineering,
School of Engineering, The University of Edinburgh,
The King's Buildings, Edinburgh, EH9 3JL, Scotland
Tim.Stratford@ed.ac.uk

KEYWORDS: Steel, strengthening, high temperatures, fibre-reinforced polymer, adhesive, bond.

ABSTRACT
Steel beams can be strengthened in flexure using bonded FRP strengthening. This method relies critically upon the bonding adhesive. A typical two-part ambient cure epoxy adhesive used for strengthening work has a glass transition temperature between about 50ºC and 80ºC, and the stiffness and strength of the adhesive decrease at temperatures somewhat below the glass transition. This paper uses tests on steel beams strengthened with carbon fibre-reinforced polymer (CFRP) plates and ambient-cure epoxy adhesive to demonstrate that slip occur across the adhesive joint as the beams are warmed up. The consequences of this deformation are investigated by comparison with an analytical model of the joint's behaviour that takes into account the change in adhesive properties with temperature.

INTRODUCTION

Properly designed and installed fibre-reinforced polymer (FRP) strengthening often requires less installation equipment and time than other strengthening techniques such as bonded steel plates or bolted strengthening solutions. Consequently, FRP strengthening is an increasingly popular method to extend the life of steel and cast iron structures (CIRIA 2004). To enable easy installation, two-part ambient-cure epoxy resins are usually used to bond the FRP to the existing structure without the need for elevated temperature curing. These ambient-cure epoxies soften at low glass-transition temperatures of typically 50-65°C (Concrete Society 2004), which are similar to the temperatures considered during the design of steel bridges in the UK (Highways Agency 2001).

Research into the elevated temperature performance of bonded FRP strengthening has so far concentrated upon the *high* temperatures present during a fire (e.g.: Kodur, Bisby & Green 2007). This paper instead investigates *warm* temperatures (< 100°C), by examining the effect of the adhesive glass transition on steel I-beams strengthened using bonded carbon FRP (CFRP) plates. It presents both an analytical model of the adhesive behaviour and the results from a preliminary experimental study.

BOND BETWEEN THE BEAM AND STRENGTHENING PLATE AT WARM TEMPERATURES

The implications of elevated temperature for an FRP-strengthened steel beam are not obvious. The glass transition of the bonding adhesive results in a reduction in *strength*, reduction in *stiffness* and increase in *deformation capacity*. In addition to the changes in adhesive properties with temperature, CFRP and steel have very different coefficients of thermal expansion (α); consequently, *differential thermal expansion* causes high shear stresses across the adhesive joint (Denton 2001). The strength reduction and differential thermal expansion are detrimental to the strengthening, but the stiffness and deformation capacity changes could be beneficial to the overall strength of the adhesive connection between the plate and beam.

Epoxy adhesive at elevated temperatures

Figure 1 shows the glass transition behaviour of the epoxy bonding adhesive considered in this paper. This is a 2-part, ambient-cure adhesive, typical of the adhesives sold specifically for plate bonding applications. The reduction in stiffness with temperature shown in the figure was obtained by dynamic mechanical analysis (DMA) on five adhesive samples (15×10×1mm; double cantilever configuration).

The tests were conducted after 15 days' ambient cure (whereas the manufacturer specifies full cure after 5 days at 25ºC).

The glass transition is not normally characterised in full (as in Figure 1), but by a single temperature, T_g. The definition of T_g varies depending upon the phenomenon being tested (Ludwig *et al.* 2008). ISO 6721 (2002), for example, defines the glass transition temperature for DMA as the peak in the tanδ curve, which is (simplistically) the ratio of plastic deformation to elastic deformation. The ISO 6721 method gives T_g = 65ºC for the current adhesive, but at this temperature the stiffness of the adhesive is less than 10% of its ambient value. Far smaller reductions in stiffness are usually important in design, and structural engineers often consider a 5% reduction in a property to be significant, which occurs at 40 ºC.

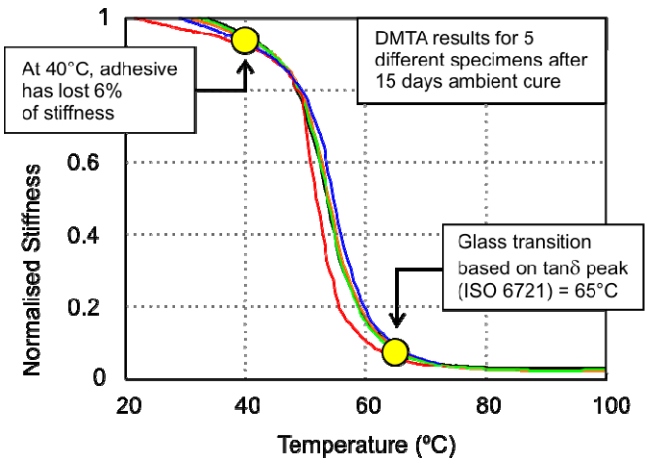

Figure 1. Measured loss in stiffness of the epoxy bonding adhesive through the glass transition.

An analytical model of adhesive bond stresses at elevated temperature

A number of researchers have proposed models that predict the distribution of bond stresses along an adhesive joint between a beam and strengthening plate (e.g.: Deng *et al.* 2004; Denton 2001; Smith and Teng 2001; Stratford and Cadei 2006). All of these models are *linear-elastic* analyses; they predict the shear and peel stress distributions within the adhesive joint. All use essentially the same analysis method, considering equilibrium and compatibility conditions across the adhesive joint.

The Appendix of this paper develops a new bond stress model that incorporates the change in adhesive properties with temperature. The analysis is similar to previous elastic analyses, but uses the adhesive constitutive response shown in Figure 2. The adhesive is idealised as an elasto-plastic material, with a shear modulus (G) and shear strength (τ_u) that reduce with temperature. At ambient temperature, the adhesive is brittle, but at elevated temperatures the adhesive undergoes plastic deformation before rupture, modelled by a horizontal plastic plateau. The stiffness and strength of the adhesive are deduced from the glass transition data in Figure 2, but data is not currently available for the strain capacity of the adhesive. Rupture is not captured in the current bond model; however, it will be seen below the strain capacity of the adhesive does not necessarily govern failure.

It should be noted that the constitutive model in Figure 3 does not capture the full complexity of the adhesive response at elevated temperatures; in particular, it does not consider time-dependent effects such as adhesive creep, or the glass transition temperature increasing due to post-cure heating. The bond stress analysis implementation in the Appendix also includes idealisations; the steel beam is assumed to remain elastic (valid for the case considered below), and a simplified boundary condition is applied at the centre of the beam.

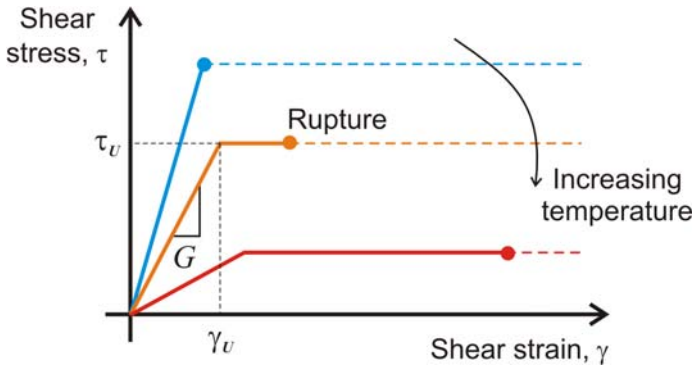

Figure 2. Simplified elasto-plastic adhesive material model.

TESTS ON CFRP STRENGTHENED STEEL BEAMS

Two-metre span steel I-beams were strengthened using bonded CFRP and tested under a combination of load and heat. The arrangement, dimensions and key properties of the beams are shown in Figure 3, with manufacturer's data sheet values for the CFRP plate and epoxy. Load was applied in inverted 4-point bending, allowing one end of the strengthening plate to be heated from above using an electrical heating pad. The temperature of the steel flange of the beam was recorded near to the end of the plate.

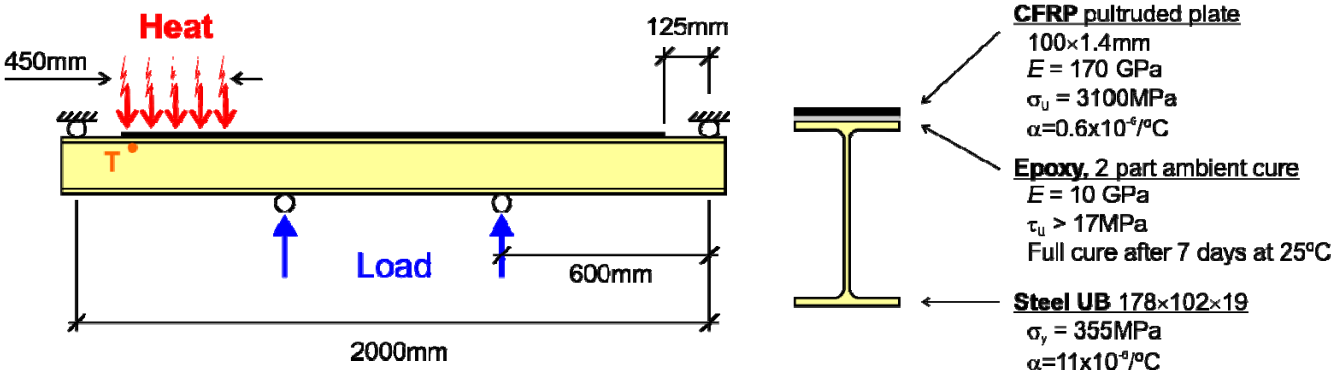

(a) Loading and heating arrangement

(b) Cross-sectional dimensions and material properties of the strengthened beams.

Figure 3. The CFRP-strengthened steel beams examined in this paper.

Table 1 summarises the tests conducted. Tests (1) and (7) determined the capacities of an unstrengthened and a strengthened beam at ambient temperature; both failed by lateral-torsional buckling and thus remained elastic up to failure. Beams 2 to 5 were first loaded to above their unstrengthened capacity. This load was held constant whilst the temperature in the adhesive was increased, until the adhesive joint failed and the plate debonded from the beam.

High-resolution digital images of the heated end of the plate were recorded at 10 second intervals. The side of the CFRP, adhesive and beam flange were first painted with a high-contrast texture, as shown in Figure 4. The images were analysed using a bespoke image-processing algorithm (White *et al.* 2003) to determine the slip (shear displacement) across the adhesive joint (Figure 5).

Additional details of the experiments can be found in Stratford and Bisby (2010).

Table 1. Details of the experimental program and headline results.

Test ID	Load (kN)	Temperature (ºC)	Comment
1	**190.0**	Ambient	Capacity of a strengthened beam (l.t. buckling)
7	**140.4**	Ambient	Capacity of an unstrengthened beam (l.t. buckling)
2	150	**65**	Plate debonding failure
4a	170	**74**	Plate debonding failure.
4b	170	**74**	Plate debonding failure.
5a	180	**60**	Plate debonding failure.
5b	180	**64**	Plate debonding failure.

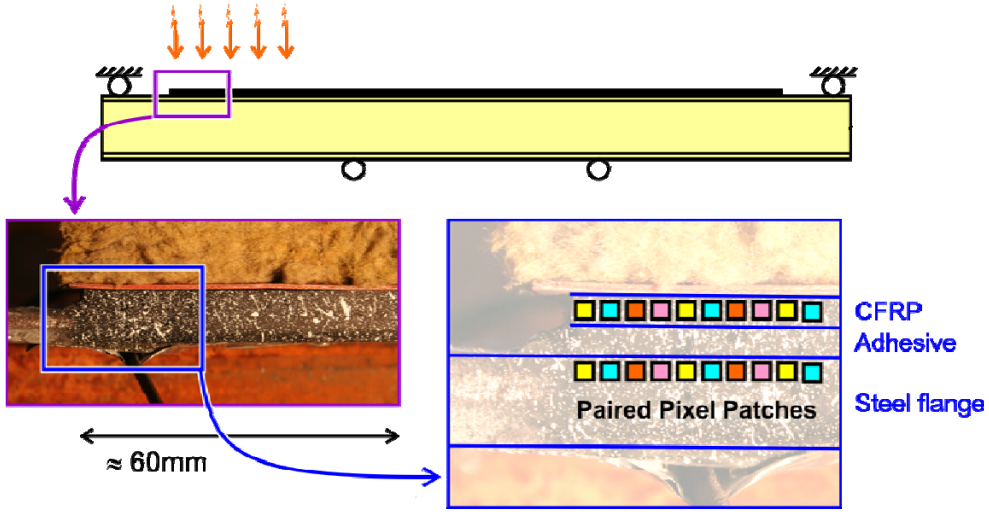

Figure 5. Measurement of slip displacements across the adhesive joint by digital image analysis.

Experimental results

The strengthening failed adhesively at the adhesive-steel interface in all tests, at the adhesive temperatures given in Table 1.

An example of the output from the image analysis is shown in Figure 6 for Test 5B. This plots the slip displacement with position from the plate end and against temperature. Significant slip displacement occurred from 40°C, and this slip increased until failure at 64°C. Slip occurs along the whole of the observed length of the adhesive joint. At temperatures of around 40°C, the slip increases towards the centre of the beam. This is counter-intuitive, but is believed to be the result of non-uniform temperature within the adhesive joint (due to conduction of heat away from the plate end).

Figure 7 plots the plate-end slip displacements for all of the tests. All tests showed similar behaviour, with large slip displacements at temperatures below 65°C (the glass transition temperature obtained using ISO 6721). The slips recorded by the last image before failure were in the range 0.16 to 0.23mm; the actual failure slip will have been slightly higher as the last image was taken up to 10 seconds prior to failure. There is no discernible trend between the failure temperature and applied load.

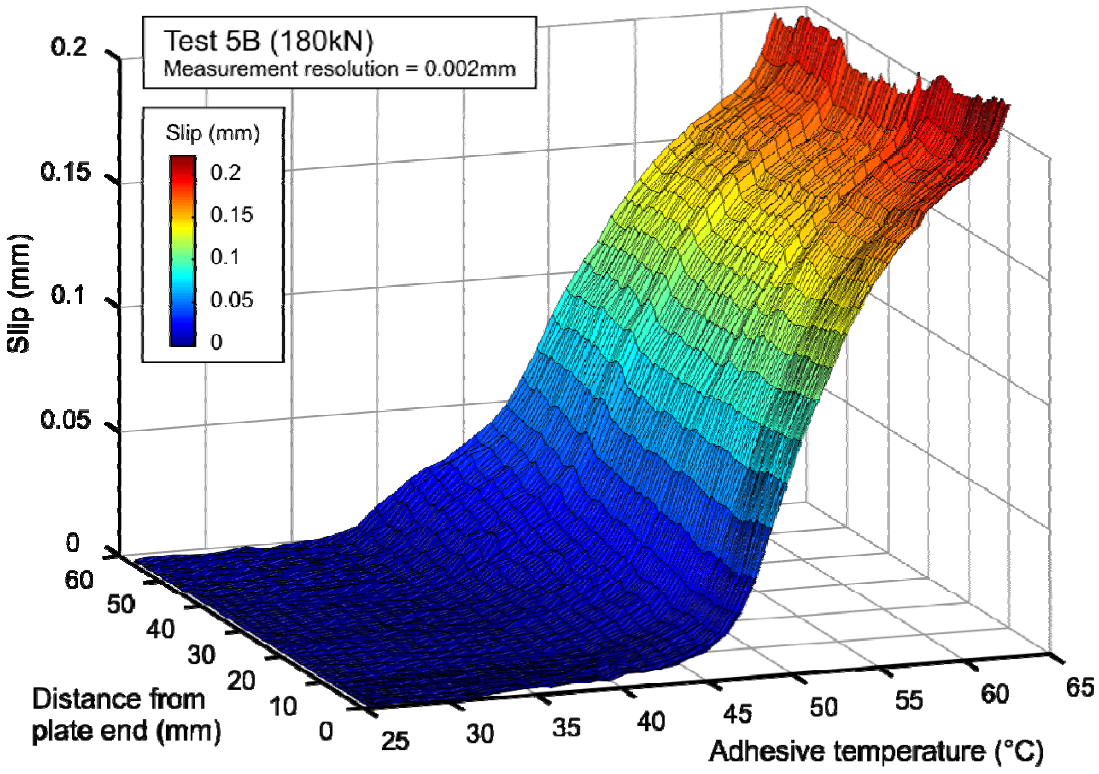

Figure 6. Variation in slip distribution with temperature for Test 5B.

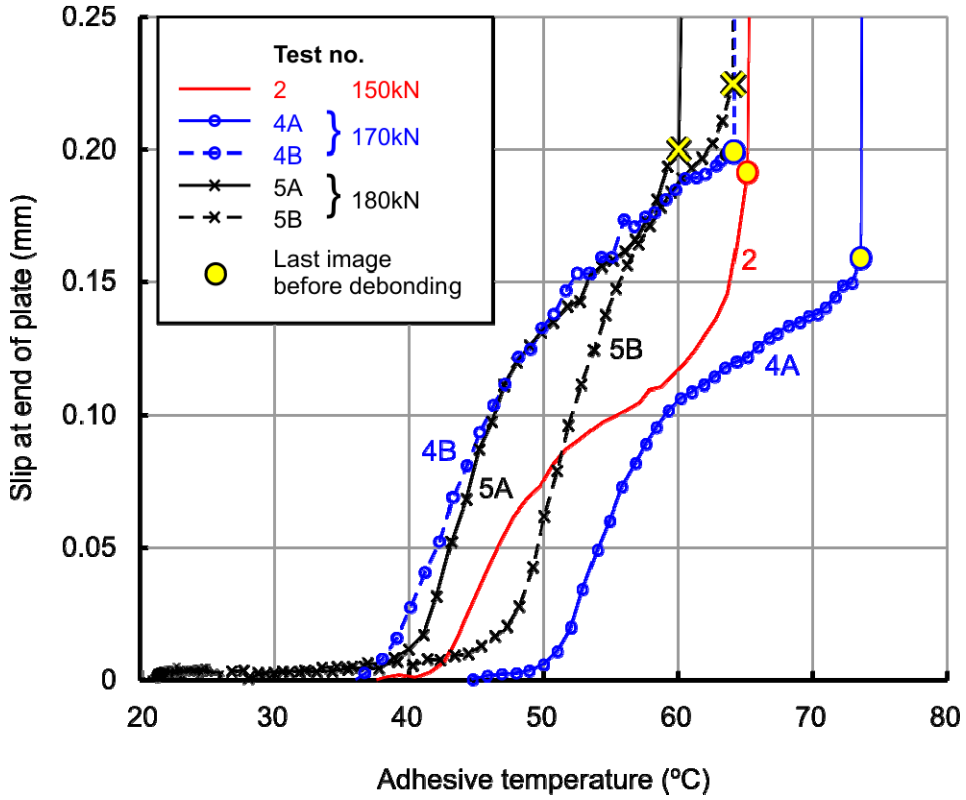

Figure 7. Plate end slip variation with temperature from the tests.

ANALYTICAL RESULTS

The elevated temperature adhesive bond stress analysis described above was used to analyse the test beams. The model used the specimen geometry and properties shown in Figure 3, except that uniform adhesive temperature was applied along the beam. The manufacturer's data sheet values were used for adhesive stiffness and strength, coupled with the DMA curve (Figure 1) for reduction in stiffness and strength with temperature. No experimental results other than the DMA curve were used as inputs for to the analysis.

Figure 8 plots the plate end slip predicted by the bond analysis for different applied loads. As observed in the tests (Figure 7), significant slip deformation occurs from around 40°C, and increases rapidly to failure. The difference in the shape of the experimental and analytical plate end slip responses is due to the model simplifications; the use of uniform heating in the model means that there is no stiffening due to the cool region beyond the heated area, nor does the simplified boundary condition in the analysis model stiffening at the centre of the beam.

The predicted failure temperature for applied loads of 150kN and 180kN is around 60°C. Whilst the slip at which failure occurs will depend upon the rupture strain of the adhesive (which is not modelled), the failure temperature is not sensitive to the rupture strain, due to the runaway nature of the failure.

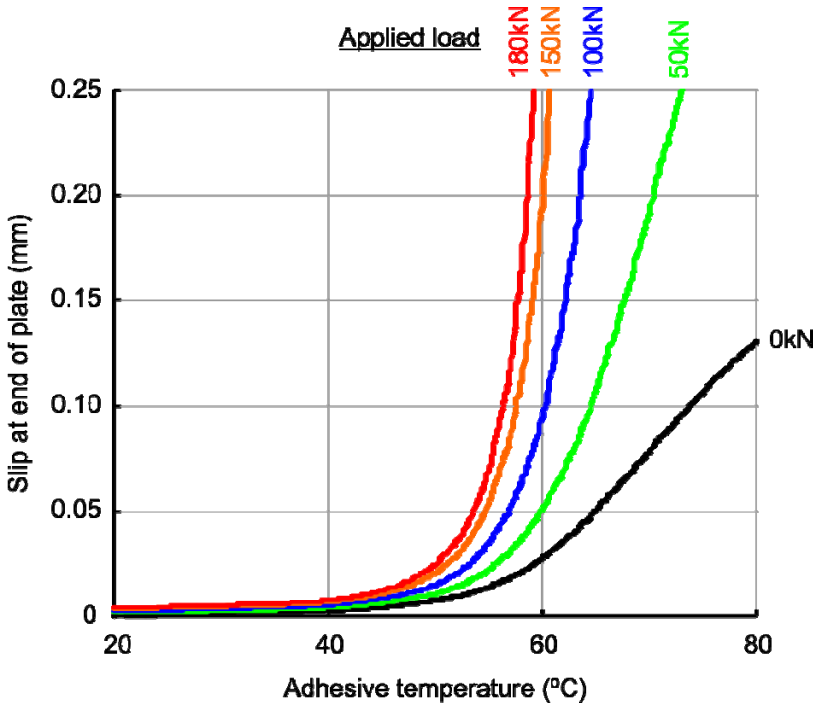

Figure 8. Plate end slip predictions from the bond analysis.

Figure 9 examines the different components of adhesive joint behaviour at elevated temperature, by plotting the plate end slip response:

- with and without an applied load of 150kN;
- with and without differential thermal expansion (DTE); and
- with and without adhesive properties that change with temperature.

The figure shows that all of the effects are important, and the complex interaction between these effects.

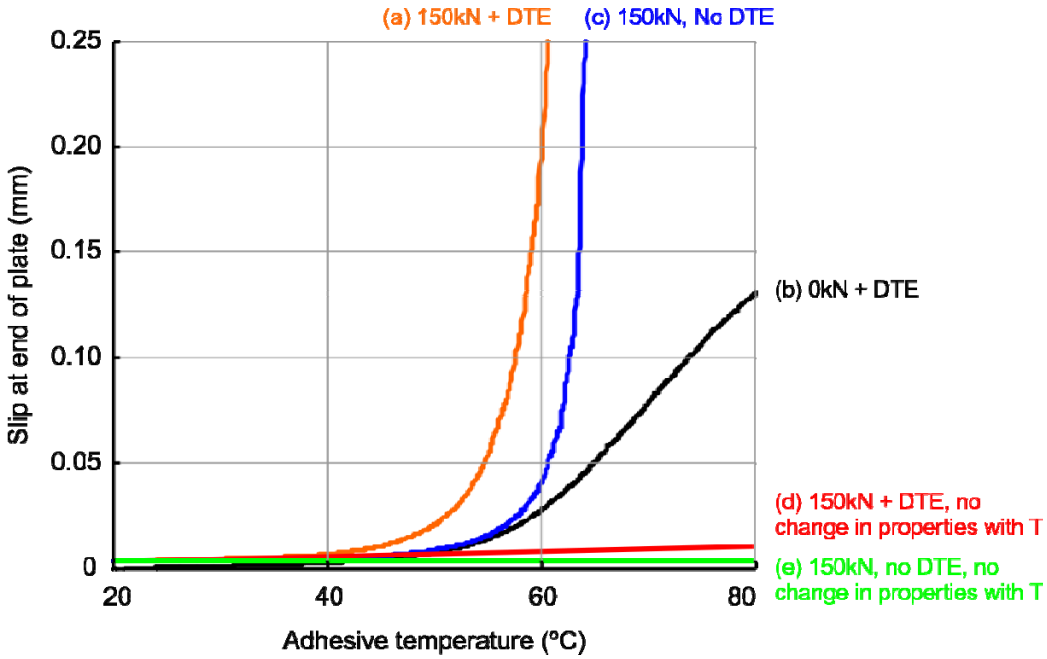

Figure 9. Plate end slip predictions from the bond analysis.

The behaviour of the adhesive joint for an applied load of 150kN is examined in more detail in Figures 10 and 11. Figure 10 plots the shear strain (γ_a) distribution at different temperatures. At low temperatures, shear strain only occurs close to the end of the plate. As the temperature increases, both the stiffness and strength of the adhesive reduce, and the region over affected by shear strain grows along the beam.

The effect of the reduction in adhesive strength with temperature is more apparent in Figure 11, which plots shear stress distributions at different temperatures. At low temperatures, the adhesive is elastic (the peak stress is highest at 40°C due to differential thermal expansion). As the temperature increases, the adhesive near the end of the plate becomes plastic, and this plastic zone spreads along the beam as the adhesive softens with increasing temperature.

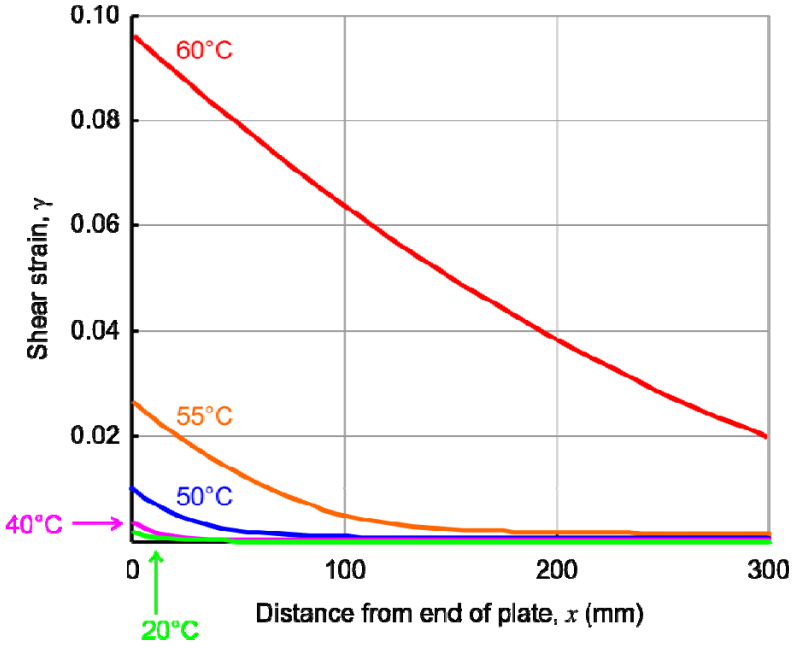

Figure 10. Shear strain distributions for 150kN applied load.

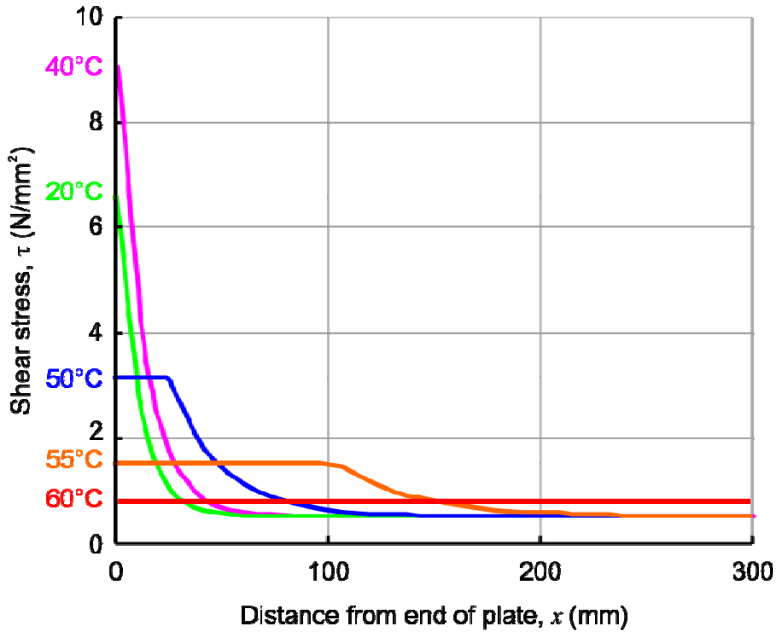

Figure 11. Shear stress distributions for 150kN applied load.

CONCLUSIONS

The test results presented in this paper demonstrate that warm temperatures can significantly reduce the strength of an FRP-plated steel beam. Irrecoverable slip deformation occurs across the adhesive joint prior to failure due to the glass transition of the adhesive. Significant slips were observed from ≈ 40°C, which is substantially below the ISO 6721 glass transition temperature of the adhesive (65ºC).

The glass transition that occurs when the strengthened beam is heated results in a weaker adhesive; however, the adhesive is also less stiff and has a greater deformation capacity. Thus, load is transferred between the strengthening plate and the flange of the beam over a longer bond length than at ambient temperature, and it is not straightforward to predict the consequences of the adhesive glass transition upon the strengthened beam.

A bond analysis has been presented in this paper that predicts the behaviour of a bonded joint at elevated temperatures, based upon the adhesive glass transition response obtained using dynamic thermal analysis (DMA) testing. The analytical results show promising agreement with the experimental results; however, additional work is required to investigate the strain capacity of the adhesive at elevated temperatures, and time dependent effects.

ACKNOWLEDGEMENTS

The experiments were undertaken by Cameron Gillespie and Martin Moran for their MEng theses, and the School of Engineering at the University of Edinburgh is thanked for its support of these projects. The Scottish Funding Council is acknowledged for its support of the Joint Research Institute, part of the Edinburgh Research Partnership in Engineering and Mathematics (ERPem). Bisby gratefully acknowledges the support of the Ove Arup Foundation and the Royal Academy of Engineering.

APPENDIX: ANALYSIS OF ADHESIVE BOND STRESS AT ELEVATED TEMPERATURES

Much of this derivation is similar other bond analyses (such as Stratford and Cadei 2006), so only a compact derivation is presented in this Appendix. The bond analysis establishes the distribution of shear stress (τ_a) along the adhesive joint; this analysis does not examine the adhesive peel stress, σ_a. Figure A1 defines many of the problem's parameters.

The adhesive stress results from applied load (resulting in an axial force N and moment M within the beam) and a uniform change in temperature (T-T_0). Internally, load is shared between the beam (N_b, M_b) and the strengthening plate (N_s, M_s). The steel beam is defined by its cross-sectional area (A_b), second moment of area (I_b), position of the neutral axis relative to the bottom fibre (y_b), Young's modulus (E_b) and coefficient of thermal expansion (α_b); the strengthening plate by A_s, I_s, y_s, E_s & α_s; and the adhesive by its thickness (t_a) and material properties from Figure 3.

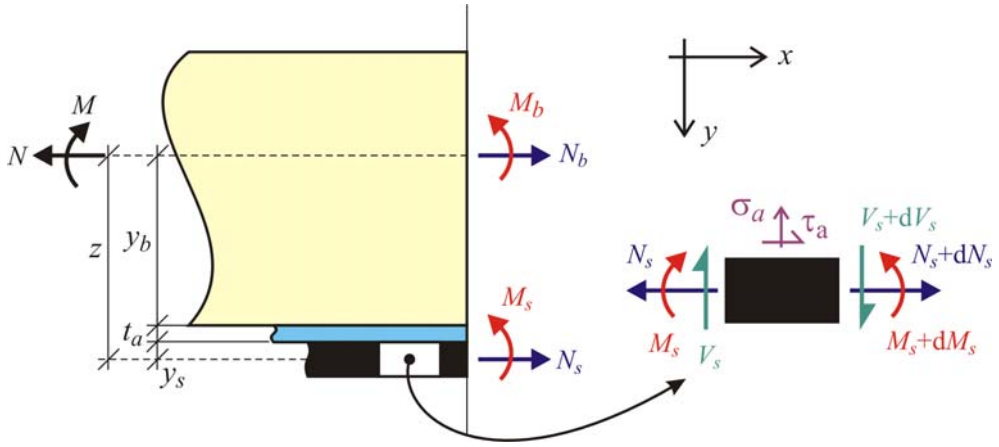

Figure A1. Beam, adhesive and strengthening plate definitions.

Derivation of the governing equation for adhesive shear stress

Equilibrium of the beam and plate with the applied loads:

$$N = N_b + N_s \tag{1}$$

$$M = M_b + M_s + N_s z \tag{2}$$

Shear compatibility across the adhesive joint (Stratford and Cadei 2006):

$$t_a \frac{d\gamma_a}{dx} = \left[\frac{1}{E_s A_s} + \frac{1}{E_b A_b} + \frac{z y_b}{E_b I_b}\right] N_s + \left[\frac{y_b}{E_b I_b} - \frac{y_s}{E_s I_s}\right] M_s + (\alpha_s - \alpha_b)(T - T_0) - \frac{N}{E_b A_b} - \frac{M y_b}{E_b I_b} \tag{3}$$

Uncouple N_s and M_s by assuming that the strengthening plate bending moment is zero (M_s=0) (Deng *et al.*, 2004):

$$t_a \frac{d\gamma_a}{dx} = \frac{k}{b_a} N_s + (\alpha_s - \alpha_b)(T - T_0) - \frac{N}{E_b A_b} - \frac{M y_b}{E_b I_b} \tag{4}$$

where:

$$k = b_a \left[\frac{1}{E_s A_s} + \frac{1}{E_b A_b} + \frac{z y_b}{E_b I_b}\right] \tag{5}$$

Differentiating gives:

$$t_a \frac{d^2\gamma_a}{dx^2} = \frac{k}{b_a} \frac{dN_s}{dx} - \frac{y_b}{E_b I_b} \frac{dM}{dx} \tag{6}$$

The shear stress is related to the change in the plate force (axial equilibrium of the plate):

$$\tau_a = \frac{1}{b_a}\frac{dN_s}{dx} \tag{7}$$

Hence, the governing equation for adhesive shear stress is:

$$t_a \frac{d^2\gamma_a}{dx^2} = k\,\tau_a - \frac{y_b}{E_b I_b}\frac{dM}{dx} \tag{8}$$

Boundary conditions

By symmetry, the shear strain at the centre of the beam ($x = L$) is zero ($\gamma_a = 0$) $\Rightarrow$

$$(\gamma_a)_{x=L} = 0 \tag{9}$$

The force in the plate is zero at its end ($N_s = 0$). From eqn (4), defining the end of the plate as $x = 0$ $\Rightarrow$

$$\left(\frac{d\gamma_a}{dx}\right)_{x=0} = \frac{1}{t_a}\left[(\alpha_s - \alpha_b)(T - T_0) - \frac{N}{E_b A_b} - \frac{M y_b}{E_b I_b}\right]_{x=0} \tag{10}$$

Solution if all of the adhesive is elastic

If the adhesive is elastic ($\tau_a = G\gamma_a$ from Figure 3) all of the way along the adhesive joint:

$$t_a \frac{d^2\gamma_a}{dx^2} = kG\gamma_a - \frac{y_b}{E_b I_b}\frac{dM}{dx} \tag{11}$$

The solution where the adhesive is elastic is:

$$\gamma_a = C_1 e^{-\lambda x} + C_2 e^{+\lambda x} + \frac{y_b}{kGE_b I_b}(M_1 + 2M_2 x) \tag{12}$$

$$\text{where } \lambda = \sqrt{\frac{kG}{t_a}} \tag{13}$$

$$\text{and the applied moment is written } M = M_0 + M_1 x + M_2 x^2 \tag{14}$$

Set $C_2 = 0$ so that $\gamma_a \to 0$ as $x \to L$, the first boundary condition (eqn 9). This is a slight approximation.

To satisfy the second boundary condition (eqn 10):

$$C_1 = \frac{1}{\lambda}\left\{\frac{2M_2 y_b}{kGE_b I_b} - \frac{1}{t_a}\left[(\alpha_s - \alpha_b)(T - T_0) - \frac{N}{E_b A_b} - \frac{y_b M_0}{E_b I_b}\right]\right\} \tag{15}$$

Solution if the adhesive is elasto-plastic

The maximum adhesive strain occurs at the plate end, thus the adhesive will first become plastic at the plate end. The adhesive will be plastic over a length p (which needs to be determined) from the end of the plate. The adhesive outside this length (towards the centre of the beam) will remain elastic.

Where the adhesive is plastic ($\tau_a = \tau_u$ from Figure 3):

$$t_a \frac{d^2\gamma_a}{dx^2} = k\tau_u - \frac{y_b}{E_b I_b}\frac{dM}{dx} \tag{15}$$

The solution where the adhesive is plastic is:

$$\gamma_a = \frac{1}{t_a}\left\{\left(k\tau_u - \frac{y_b M_1}{E_b I_b}\right)\frac{x^2}{2} - \frac{M_2 y_b}{3E_b I_b}x^3\right\} + C_3 x + C_4 \tag{16}$$

At the end of the plate (eqn 10) the adhesive is plastic $\Rightarrow$

$$C_3 = \frac{1}{t_a}\left[(\alpha_s - \alpha_b)(T - T_0) - \frac{N}{E_b A_b} - \frac{M_0 y_b}{E_b I_b} \right] \tag{17}$$

The division between the plastic and elastic zones occurs at $x = p$, and the shear strain at this position is $\gamma_a = \gamma_u$.

$$C_4 = \gamma_u - \frac{1}{t_a}\left\{ \left(k\tau_u - \frac{y_b M_1}{E_b I_b} \right)\frac{p^2}{2} - \frac{M_2 y_b}{3E_b I_b} p^3 \right\} - C_3 p \tag{18}$$

The adhesive towards the centre of the beam is elastic, so is governed by eqn (12). Use $C_2 = 0$ as above.

At the interface between the elastic and plastic zones, $x = p$ and $\gamma_a = \gamma_u$:

$$C_1 e^{-\lambda p} = \gamma_u - \frac{y_b}{kGE_b I_b}(M_1 + 2M_2 p) \tag{19}$$

The force in the plate (N_s) must be equal between the elastic and plastic zones, requiring continuity in $d\gamma_a/dx$ at $x = p$:

$$-C_1 \lambda e^{-\lambda p} + \frac{2M_2 y_b}{kGE_b I_b} = \frac{1}{t_a}\left\{ \left(k\tau_u - \frac{y_b M_1}{E_b I_b} \right) p - \frac{M_2 y_b}{E_b I_b} p^2 \right\} + C_3 \tag{20}$$

Combining (19) and (20) gives a quadratic equation for p:

$$0 = \frac{M_2 y_b}{t_a E_b I_b} p^2 + \left(\frac{2M_2 \lambda y_b}{kGE_b I_b} + \frac{y_b M_1}{t_a E_b I_b} - \frac{k}{t_a}\tau_u \right) p + \left(\frac{\lambda y_b M_1 + 2M_2 y_b}{kGE_b I_b} - \lambda \gamma_u - C_3 \right) \tag{21}$$

Eqns 17, 18, 19 and 21 between them define the boundary coefficients (C_2, C_3, C_4) and the interface position (p); thus, the shear strain distribution can be completely defined.

The shear strain at the end of the plate ($x = 0$) is given by:

$$(\gamma_a)_{x=0} = C_1 + \frac{y_b M_1}{kGE_b I_b} \qquad \text{if all the adhesive is elastic} \tag{22}$$

or $$(\gamma_a)_{x=0} = C_4 \qquad \text{if a plastic zone exists in the adhesive} \tag{23}$$

The slip deformation can be found from the shear strain as:

$$s = t_a \gamma_a \tag{24}$$

REFERENCES

CIRIA (2004). *Strengthening metallic structures using externally bonded fibre-reinforced polymers.* C595, CIRIA, London, UK.

Concrete Society (2004), *Design Guidance for Strengthening Concrete Structures using Fibre Composite Materials,* Technical Report 55, 2nd Edition, The Concrete Society, Camberley, UK.

Deng J., Lee M.M.K. and Moy S.S.J. (2004). *Stress analysis of steel beams reinforced with a bonded CFRP plate,* Composite Structures, 65, 205–15.

Denton SR. (2001). *Analysis of stresses developed in FRP plated beams due to thermal effects.* 1st International Conference on FRP Composite in Civil Engineering, 527–536.

Highways Agency. (2001). BD37/01: *Loads for Highways Bridges. Design Manual for Roads and Bridges.* The Stationary Office Ltd., London, UK.

IS0 6721-1:2002. *Plastics. Determination of dynamic mechanical properties. General principles*. BSI, London, UK.

Kodur, V.K.R., Bisby, L.A. and Green, M.F. (2007). *Preliminary guidance for the design of FRP-strengthened concrete members Bonded Fibre Reinforced Polymer Strengthening exposed to fire,* Journal of Fire Protection Engineering, 17(5), 5–26

Ludwig C., Knippers J., Hugi E., and Ghazi Wakili K. (2008). *Damage of flexural loaded composite beams subjected to fire.* 4th International Conference on FRP Composites in Civil Engineering, 527–536.

Smith S.T. and Teng J.G. (2001). *Interfacial stresses in plated beams*. Engineering Structures 2001, 23, 857–871.

Stratford T. and Cadei J. (2006). *Elastic analysis of adhesion stresses for the design of a strengthening plate bonded to a beam,* Construction and Building Materials, 20, 34-45

Stratford T.J. and Bisby L.A. (2010). *Temperature Effects in Adhesively Bonded FRP Strengthening Applied to Steel Beams: Experimental Observations.* 5th International Conference on FRP Composites in Civil Engineering, Beijing, September 2010.

White D.J., Take W.A. and Bolton M.D. (2003). *Soil deformation measurement using particle image velocimetry (PIV) and photogrammetry*. Geotechnique 53(7), 619-631